# Comparative Study of C-H Stretch and Bend Vibrations in Methane Activation on Ni(100) and Ni(111)

L. B. F. Juurlink
*Leiden Institute of Chemistry, Gorlaeus Laboratories, Leiden University, 2300 RA Leiden, The Netherlands*

R. R. Smith, D. R. Killelea, and A. L. Utz
*Department of Chemistry and W. M. Keck Foundation Laboratory, Tufts University, Medford, Massachusetts 02155, USA*
(Received 2 December 2004; published 25 May 2005)

State-resolved measurements on clean Ni(100) and Ni(111) surfaces quantify the reactivity of $CH_4$ excited to $v = 3$ of the $\nu_4$ bend vibration. A comparison with prior data reveals that $3\nu_4$ is significantly less effective than the $\nu_3$ C-H stretch at promoting dissociative chemisorption, even though $3\nu_4$ contains 30% more energy. These results contradict statistical theories of gas-surface reactivity, provide clear evidence for vibrational mode specificity in a gas-surface reaction, and point to a central role for C-H stretching motion along the reaction path to dissociative chemisorption.

DOI: 10.1103/PhysRevLett.94.208303 PACS numbers: 82.20.Bc, 68.35.Ja, 68.49.Df, 82.65.+r

Vibrationally excited molecules can play a central role in gas-phase reactions, and recent state-resolved studies are revealing that these energized molecules may play a similarly important role in gas-surface reactivity [1–4]. Despite their importance in reactive environments, key questions regarding their dissociative chemisorption dynamics remain [5]. Here, we use an experimental approach that quantifies the reaction probability, $S_0$, of molecules in select vibrational states. We compare $S_0$ for $CH_4$ molecules containing two distinct types of vibrational excitation—an antisymmetric C-H stretch ($S_0^{\nu_3}$) and three quanta of the triply degenerate bending vibration ($S_0^{3\nu_4}$). Our data reveal that the more energetic $3\nu_4$ state is less reactive than $\nu_3$ on both Ni(100) and Ni(111). These results offer the first direct comparison of C-H stretch and bend excitation in promoting $CH_4$ dissociation on a metal, establish the relative importance of C-H stretching and bending motion in promoting transition state access in this prototypical gas-surface reaction, and provide further evidence for nonstatistical, mode selective behavior in dissociative chemisorption on metal surfaces.

Methane dissociation on nickel is highly activated [6]. $S_0$ increases exponentially as translational energy ($E_{\text{trans}}$) and average vibrational energy ($E_{\text{vib}}$) increase [4,7,8]. Empirical and *ab initio* potential energy surfaces have a ''late'' barrier for dissociation [9–11]. Transition state calculations predict a significantly elongated active C-H bond that is bent relative to the $C_3$ axis of the nonreactive methyl group [12]. These findings point to important roles for both $E_{\text{trans}}$ and $E_{\text{vib}}$ in $CH_4$ activation.

The nature of methane's vibrational activation has been debated for many years. Early beam-surface scattering experiments established the importance of $E_{\text{vib}}$ [7], but it has remained unclear which of methane's many vibrational modes were responsible for the activation—or whether all modes contributed equally. Collision induced dissociation measurements on Ni(111) suggested a key role for bending vibrations [13], but reduced dimensionality transition state calculations pointed to the importance of C-H stretching motion in accessing the transition state [9]. An empirical model that attributed all vibrational activation to a pseudodiatomic C-H oscillator successfully reproduced both beam and bulb measurements of $CH_4$ dissociation on Ni(100) [10]. Wave-packet calculations predicted vibrational-state-dependent differences in the coupling of $E_{\text{vib}}$ to the surface [14]. The authors postulated that this effect could lead to mode specific reactivity, with C-H stretching states being most reactive. In contrast, a statistical model based on microcanonical unimolecular rate theory assumed equal reactivity on a per-energy basis for all $CH_4$ vibrational states and has successfully reproduced much of the experimental data for dissociation on Ni [15] and Pt [16] surfaces. Controversy persists because $S_0$ values averaged over the many vibrational states present in a typical $CH_4$ sample can obscure key details of the system's dynamical behavior.

This Letter describes experiments that quantify $S_0^{3\nu_4}$. The molecules impinge on clean Ni(100) or Ni(111) surfaces along the surface normal. High-level anharmonic force field calculations indicate that the $3\nu_4$ eigenstate we excite with our laser is nearly identical to a zero-order bending normal mode and that the laser-prepared $\nu_3$ eigenstate is nearly identical to a zero-order C-H stretch normal mode state [17]. We can therefore compare $S_0$ for $3\nu_4$ with previously published data for $\nu_3$ [4,18] to understand how C-H stretch and bend excitation promote $CH_4$ dissociation on low-index Ni surfaces.

We performed the experiments in a triply differentially pumped supersonic molecular beam-surface scattering apparatus [19]. A 2% mixture of $CH_4$ in $H_2$ expanded continuously from a 294, 400, 500, 550, or 600 K nozzle and formed the molecular beam. Infrared (IR) light from a

 © 2005 The American Physical Society

continuous wave, single mode laser intersected the molecular beam and excited a fraction of the molecules to $J = 2$ of the $F_2$ symmetry $3\nu_4$ vibration via the R(1) transition at 3876.7771 $cm^{-1}$. A room temperature pyroelectric detector translated into the molecular beam quantified IR absorption. Methane's long IR radiative lifetime and collision-free conditions in the beam ensured that the optically excited molecules impinged on the 475 K Ni surface in their initially prepared state. Auger electron spectroscopy (AES) quantified carbon deposition as a signature of dissociative chemisorption. We performed all measurements in the limit of low coverage (less than 0.12 ML C) and computed $S_0$ as the quotient of carbon's areal density on the surface (as determined by AES) and the integrated incident flux of $CH_4$.

We have shown [4] that Eq. (1) yields the reaction probability for the laser-excited state $S_0^{3\nu_4}$:

$$S_0^{3\nu_4} = \frac{S_0^{\text{LaserOn}} - S_0^{\text{LaserOff}}}{f_{\text{exc}}} + S_0^{v=0}. \quad (1)$$

We measured $S_0$ for $CH_4$ in the molecular beam with and without laser excitation ($S_0^{\text{LaserOn}}$ and $S_0^{\text{LaserOff}}$, respectively) and quantified the fraction of molecules optically excited ($f_{\text{exc}}$) to calculate $S_0^{3\nu_4}$. At the energies studied here, $S_0^{v=0}$ contributes negligibly to $S_0^{3\nu_4}$.

Saturation measurements determined $f_{\text{exc}}$ in our studies of $\nu_3$ [19], but the weak $3\nu_4$ overtone transition precluded that approach here. Instead, we compared IR absorption signals for $3\nu_4$ and $\nu_3$ excitation and found $f_{\text{exc}} = 0.0024$ for the $3\nu_4$ experiments on Ni(100). Experimental improvements prior to the Ni(111) work increased $f_{\text{exc}}$ to 0.010–0.017, depending on molecular beam conditions. We independently validated our experimental measurements of $f_{\text{exc}}$ by using instrument parameters determined in our $\nu_3$ experiments, known Einstein coefficients for the $\nu_3$ and $3\nu_4$ transitions [20], and measured IR radiation densities to calculate $f_{\text{exc}}$.

When $f_{\text{exc}}$ is small, $S_0^{\text{LaserOn}}$ and $S_0^{\text{LaserOff}}$ differ little. To best quantify $S_0^{\text{LaserOn}} - S_0^{\text{LaserOff}}$, we rely on the localized deposition of laser-excited molecules on the Ni surface [21]. Figure 1 shows that molecules traveling toward the crystal edge have a transverse velocity component along the laser's propagation direction. When the laser is tuned to the center of the Doppler profile, it excites only molecules whose homogeneous linewidth overlaps with the laser's emission—i.e., those molecules traveling toward the crystal center. Molecules traveling toward the crystal edge are Doppler detuned from the laser's emission and are not excited. Spatially resolved AES measurements quantify C coverage at a series of points across the surface and allow us to measure $S_0^{\text{LaserOn}}$ (center) and $S_0^{\text{LaserOff}}$ (near edge) in a single experiment.

Carbon deposition maps from our prior studies of laser-excited $CH_4$ ($\nu_3$) incident on Ni(100) with $E_{\text{trans}} = 50$ kJ/mol appear in Fig. 2(a). In the absence of laser excitation, the uniform $CH_4$ flux in the beam results in constant C coverage across the crystal (open symbols). With laser excitation (solid symbols) C deposition is enhanced near the crystal center. The measured quantities and Eq. (1) yield $S_0^{\nu_3} = 1.8 \times 10^{-3}$.

Figure 2(b) shows carbon deposition maps for $CH_4$ ($3\nu_4$) incident on a clean, 475 K Ni(100) surface with $E_{\text{trans}} = 50$ kJ/mol. Both the $\nu_3$ and $3\nu_4$ experiments exposed each surface Ni atom to an incident flux of 26 laser-excited molecules, but the small $f_{\text{exc}}$ for $3\nu_4$ required us to increase

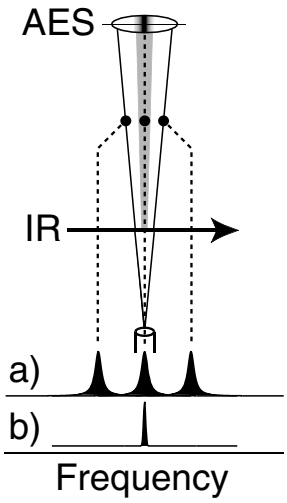


FIG. 1. Spatially localized deposition of laser-excited molecules. Molecules approach the surface in a diverging molecular beam. (a) Doppler-detuned absorption profiles for three paths. Molecules in center path absorb IR light (b) and show enhanced reactivity near the crystal center. AES spectra collected along the line shown generate data for Fig. 2.

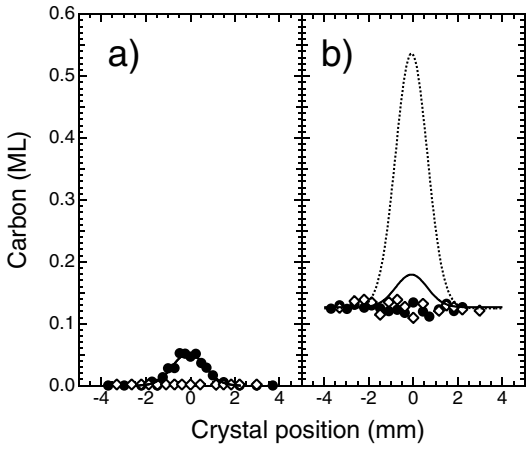


FIG. 2. Carbon deposition maps for $CH_4$ on Ni(100). (a) $\nu_3$ excitation. Laser-excited molecules near the beam center are much more reactive than the Doppler-detuned molecules. (b) The $3\nu_4$ excitation. Solid line is expected deposition profile if $3\nu_4$ and $\nu_3$ are equally reactive. Dashed line is expected deposition profile if $\eta_{\text{vib}}^{3\nu_4}$ and $\eta_{\text{vib}}^{\nu_3}$ are equal.

the dose time from 8 to 240 min, thereby increasing laser-off deposition 30-fold. Inspection of the $3\nu_4$ data reveals no detectable laser-enhanced deposition near the crystal center. Were $S_0^{\nu_3}$ and $S_0^{3\nu_4}$ equal, we would expect the carbon deposition map indicated by the solid line in Fig. 2(b). In fact, because $3\nu_4$ is more energetic than $\nu_3$, statistical theories would predict $S_0^{3\nu_4}$ to be significantly greater than $S_0^{\nu_3}$. The dashed line in Fig. 2(b) shows the expected carbon deposition map if $\nu_3$ and $3\nu_4$ were equally reactive on a per-energy basis. We conclude that at $E_{\text{trans}} = 50$ kJ/mol, $S_0^{3\nu_4} \leq 5 \times 10^{-4}$—at least 4 times less reactive than $\nu_3$. Measurements at $E_{\text{trans}} = 9.9$ kJ/mol also failed to detect laser-enhanced reactivity.

We next studied the reactivity of $CH_4$ ($3\nu_4$) incident on Ni(111) and were able to quantify $S_0^{3\nu_4}$ over a wide range of $E_{\text{trans}}$, as shown in Fig. 3. Our ability to quantify $S_0^{3\nu_4}$ on Ni(111) but not on Ni(100) is consistent with prior work in which we found vibrational activation by $\nu_3$ to be more pronounced on Ni(111) [18] than on Ni(100) [4]. Each point in Fig. 3 represents the average of at least three individual experiments. The vanishing difference between $S_0^{\text{LaserOn}}$ and $S_0^{\text{LaserOff}}$ prevented us from extending the $E_{\text{trans}}$ range of the data beyond that shown. Experimental data and curves for $S_0^{\nu_3}$ and $S_0^{v=0}$ from a previous report appear for comparison [18]. Measurements of $S_0^{\text{LaserOff}}$ (open circles) are upper limits on $S_0^{v=0}$. The curve passing near $S_0^{\text{LaserOff}}$ represents our best estimate of $S_0^{v=0}$ [18]. On Ni(111), $3\nu_4$ molecules are up to 60-fold more reactive than those in $v = 0$ and about half as reactive as $\nu_3$ molecules at all $E_{\text{trans}}$ investigated.

Close examination of the $S_0$ curves in Fig. 3 allows us to compare how $E_{\text{trans}}$ and $E_{\text{vib}}$ in $\nu_3$ and $3\nu_4$ activate $CH_4$ dissociation. Our experiments select the internal quantum state of the incident $CH_4$ molecules, their speed and direction of travel. Other important dynamical variables, including the surface impact site, the relative phase of the $CH_4$ vibration upon impact, the phase and amplitude of surface phonons, and the orientation of the active C-H bond, influence reaction energetics but lie beyond experimental control. The ensemble of $CH_4$ molecules incident on the surface samples a wide range of these dynamical variables, which leads to a distribution of $E_{\text{trans}}$ thresholds for reaction [22]. $S_0$ measured at a particular $E_{\text{trans}}$ reveals the fraction of the ensemble whose reaction threshold is $\leq E_{\text{trans}}$. Plots of $S_0$ vs $E_{\text{trans}}$ in Fig. 3 are cumulative integrals of the effective reactive barrier height distribution along the $E_{\text{trans}}$ coordinate. If $E_{\text{vib}}$ reduces the need for $E_{\text{trans}}$ by a constant amount without altering the shape of the distribution, then different vibrational states will have $S_0$ curves with an identical shape, but varying offset along the $E_{\text{trans}}$ axis. The ratio of $E_{\text{vib}}$ to the $E_{\text{trans}}$ offset is $\eta_{\text{vib}}$, a measure of vibrational efficacy that is grounded in the system's energetics and applicable at all $E_{\text{trans}}$ and $S_0$.

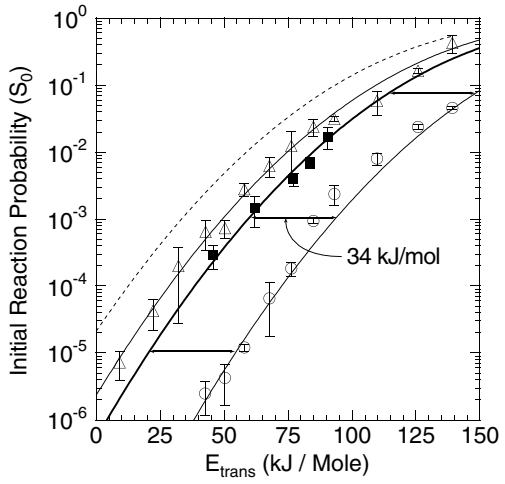


FIG. 3. State-resolved $S_0$ for $CH_4$ molecules incident on Ni(111) in $v = 0$ (circles), $\nu_3$ (triangles), and $3\nu_4$ (squares). Arrows indicate the shift in $S_0^{3\nu_4}$ relative to $S_0^{v=0}$. The dashed line denotes the $S_0^{3\nu_4}$ curve expected if $\eta_{\text{vib}}^{3\nu_4}$ equaled $\eta_{\text{vib}}^{\nu_3}$.

Since the $S_0^{3\nu_4}$, $S_0^{\nu_3}$, and $S_0^{v=0}$ curves in Fig. 3 have comparable shapes, shifts of the curves along the $E_{\text{trans}}$ axis reveal how $\nu_3$ and $3\nu_4$ reduce the $E_{\text{trans}}$ requirement for reaction. The $3\nu_4$ state contains 47 kJ/mol of $E_{\text{vib}}$ and shifts $S_0^{3\nu_4}$ by 34 kJ/mol relative to $S_0^{v=0}$, leading to $\eta_{\text{vib}}^{3\nu_4} = 0.72$. This efficacy is significant and comparable to previously reported values for $D_2$ dissociation on copper [23] and $CH_4$ ($2\nu_3$) on Ni(100) [24], but is only about 60% of the $\eta_{\text{vib}}^{\nu_3} = 1.25$ reported for $CH_4$ dissociation on Ni(111) [18]. On Ni(100), a similar analysis using our upper limit on $S_0^{3\nu_4}$ indicates that $\eta_{\text{vib}}^{3\nu_4} < 0.5$ compared to $\eta_{\text{vib}}^{\nu_3} = 1.0$ on this surface. Therefore $\nu_3$ is more effective than $3\nu_4$ in promoting methane dissociation on both Ni(111) and Ni(100), despite the fact that $3\nu_4$ contains nearly 30% more $E_{\text{vib}}$. The vibrational efficacy for both states is lower on Ni(100) than it is on Ni(111).

The data in Figs. 2 and 3 provide direct evidence for vibrational mode specificity in this gas-surface reaction. In contrast to predictions of statistical theories, which presuppose rapid and full redistribution of energy in the reaction complex, we observe a less energetic mode to be more reactive. This suggests that energy flow during reaction is uniquely influenced by the initial vibrational state of the gas-phase $CH_4$ molecule. Such behavior has a precedent in $CH_4$ dissociation on Ni. Beck *et al.* studied $CH_2D_2$ dissociation on Ni(100), and reported that two C-H stretch quanta in a localized C-H bond mode were 5 times more reactive than a more energetic state whose quanta were shared among the C-H bonds [25]. Our comparison of $E_{\text{vib}}$ and $E_{\text{trans}}$ in $CH_4$ ($\nu_3$) activation on Ni(111) revealed nonstatistical behavior too [18].

We suggest three possible origins for the nonstatistical behavior we observe. First, $\nu_3$ may better couple to the reaction coordinate. Such behavior is consistent with dynamical predictions of the "Polanyi rules" when applied to a gas-surface potential energy surface with many vibra-

tional coordinates [26]. Second, $\nu_3$ and $3\nu_4$ may differ in their coupling to the substrate. Energy transfer propensity rules for $E_{vib}$ predict more facile quenching of small (i.e., $\nu_4$) quanta by low-frequency surface phonons. Such energy loss channels compete with reactive channels for available $E_{vib}$. Finally, state-resolved studies of $D_2$ on Cu [23] and $CH_4$ on Ni(100) [4,24] ) show that $\eta_{vib}$ for overtone states are less than that of the vibrational fundamental. Further study may reveal that $\eta_{vib}$ for $\upsilon = 1$ of $\nu_4$ exceeds $\eta_{vib}^{3\nu_4}$.

Our results impact the comparison of $CH_4$ dissociation data from beam and bulb experiments. Stretch quanta in $CH_4$ contain nearly twice the energy of C-H bend quanta, so $CH_4$ vibrations group into polyads of energetically similar states. Within each polyad, bending states are least energetic, and stretching states most energetic. High collision numbers in a bulb ensure thermal population of all vibrations, but vibrational cooling in a molecular beam is limited and produces a highly nonthermal vibrational state distribution [27]. The dominant V-T energy transfer channels in a beam favor small $\Delta E_{vib}$, which serves to transfer population within each polyad to the lowest energy, or bending states [27]. The results presented here suggest that bending states may be significantly less reactive than C-H stretching states in the same polyad. Therefore, $S_0$ measurements made with the vibrational state distribution present in a supersonic molecular beam of $CH_4$ are biased toward the reactivity of bending states and likely underestimate the reactivity of a thermal vibrational state distribution, especially at low $E_{trans}$ where $S_0$ varies most between excited vibrational states.

These data deepen our understanding of vibrational activation in $CH_4$ dissociation. First, both C-H stretching and bending vibrations contribute significantly to reactivity. Reduced dimensionality models that attribute all vibrational activation to C-H stretching states either will miss a significant source of reactivity present in a thermal sample or will severely overestimate the reactivity of C-H stretching states. Second, we find that $\eta_{vib}^{\nu_3}$ significantly exceeds $\eta_{vib}^{3\nu_4}$ for $CH_4$ dissociative chemisorption on Ni(100) and Ni(111) suggesting that the $\nu_3$ antisymmetric C-H stretch coordinate is more effective than a C-H bending state ($3\nu_4$) at moving reagents toward the transition state for reaction. Third, even though we find $3\nu_4$ to be less reactive than $\nu_3$, we note that bending overtone and combination states in $CH_4$ have much higher degeneracies at a given level of vibrational excitation. Therefore, even though stretching states may be more reactive on a per-energy basis, the preponderance of excited bending states in a thermal distribution may result in bending states contributing significantly, or even dominating the reactivity of thermal distributions of methane molecules. Fourth, the data suggest that statistical theories are unreliable predictors of $S_0$ for individual states. Finally, differences in the reactivity of stretching and bending states point to complications in comparing the ensemble-averaged reactivity of nonthermal vibrational state populations in $CH_4$ beam experiments with corresponding thermally averaged quantities obtained from bulb measurements.

We gratefully acknowledge support by the National Science Foundation (CHE-0111446) and Tufts University.

[1] G. O. Sitz, Rep. Prog. Phys. **65**, 1165 (2002).
[2] D. C. Jacobs, J. Phys. Condens. Matter **7**, 1023 (1995).
[3] H. Hou, Y. Huang, S. J. Guiding, C. T. Rettner, D. J. Auerbach, and A. M. Wodtke, Science **284**, 1647 (1999).
[4] L. B. F. Juurlink, P. R. McCabe, R. R. Smith, C. L. DiCologero, and A. L. Utz, Phys. Rev. Lett. **83**, 868 (1999).
[5] A. C. Luntz, Science **302**, 70 (2003).
[6] J. H. Larsen and I. Chorkendorff, Surf. Sci. Rep. **35**, 165 (1999).
[7] M. B. Lee, Q. Y. Yang, and S. T. Ceyer, J. Chem. Phys. **87**, 2724 (1987).
[8] P. M. Holmblad, J. Wambach, and I. Chorkendorff, J. Chem. Phys. **102**, 8255 (1995).
[9] H. Yang and J. L. Whitten, J. Chem. Phys. **96**, 5529 (1992).
[10] A. C. Luntz, J. Chem. Phys. **102**, 8264 (1995).
[11] A. P. J. Jansen and H. Burghgraef, Surf. Sci. **344**, 149 (1995).
[12] P. Kratzer, B. Hammer, and J. K. Nørskov, J. Chem. Phys. **105**, 5595 (1996).
[13] J. D. Beckerle, A. D. Johnson, Q. Y. Yang, and S. T. Ceyer, J. Chem. Phys. **91**, 5756 (1989).
[14] R. Milot and A. P. J. Jansen, Phys. Rev. B **61**, 15 657 (2000).
[15] H. L. Abbott, A. Bukoski, D. F. Kavulak, and I. Harrison, J. Chem. Phys. **119**, 6407 (2003).
[16] A. Bukoski, D. Blumling, and I. Harrison, J. Chem. Phys. **118**, 843 (2003).
[17] E. Venuti, L. Halonen, and R. G. Della Valle, J. Chem. Phys. **110**, 7339 (1999).
[18] R. R. Smith, D. R. Killelea, D. F. DelSesto, and A. L. Utz, Science **304**, 992 (2004).
[19] P. R. McCabe, L. B. F. Juurlink, and A. L. Utz, Rev. Sci. Instrum. **71**, 42 (2000).
[20] L. S. Rothman *et al.*, J. Quant. Spectrosc. Radiat. Transfer **60**, 665 (1998).
[21] L. B. F. Juurlink, R. R. Smith, and A. L. Utz, J. Phys. Chem. B **104**, 3327 (2000).
[22] A. C. Luntz, J. Chem. Phys. **113**, 6901 (2000).
[23] H. A. Michelsen, C. T. Rettner, D. J. Auerbach, and R. N. Zare, J. Chem. Phys. **98**, 8294 (1993).
[24] M. P. Schmid, P. Maroni, R. D. Beck, and T. R. Rizzo, J. Chem. Phys. **117**, 8603 (2002).
[25] R. D. Beck, P. Maroni, D. C. Papageorgopoulos, T. T. Dang, M. P. Schmid, and T. R. Rizzo, Science **302**, 98 (2003).
[26] J. C. Polanyi, Acc. Chem. Res. **5**, 161 (1972).
[27] D. K. Bronnikov, D. V. Kalinin, V. D. Rusanov, Y. G. Filimonov, Y. G. Selivanov, and J. C. Hilico, J. Quant. Spectrosc. Radiat. Transfer **60**, 1053 (1998).